The Astrophysical Journal Supplement Series, 209:5 (13pp), 2013 November doi:10.1088/0067-0049/209/1/5

SUPERFLARES ON SOLAR-TYPE STARS OBSERVED WITH *KEPLER*. I. STATISTICAL PROPERTIES OF SUPERFLARES

Takuya Shibayama[1], Hiroyuki Maehara[2,3], Shota Notsu[1], Yuta Notsu[1], Takashi Nagao[1], Satoshi Honda[2,4], Takako T. Ishii[2], Daisaku Nogami[2], and Kazunari Shibata[2]
[1] Department of Astronomy, Kyoto University, Sakyo, Kyoto 606-8502, Japan; shibayama@kwasan.kyoto-u.ac.jp
[2] Kwasan and Hida Observatory, Kyoto University, Yamashina, Kyoto 607-8471, Japan
[3] Kiso Observatory, Institute of Astronomy, School of Science, The University of Tokyo, 10762-30, Mitake, Kiso-machi, Kiso-gun, Nagano 397-0101, Japan
[4] Center for Astronomy, University of Hyogo, 407-2, Nishigaichi, Sayo-cho, Sayo, Hyogo 679-5313, Japan
Received 2012 September 6; accepted 2013 August 6; published 2013 October 17

ABSTRACT

By extending our previous study by Maehara et al., we searched for superflares on G-type dwarfs (solar-type stars) using *Kepler* data for a longer period (500 days) than that (120 days) in our previous study. As a result, we found 1547 superflares on 279 G-type dwarfs, which is much more than the previous 365 superflares on 148 stars. Using these new data, we studied the statistical properties of the occurrence rate of superflares, and confirmed the previous results, i.e., the occurrence rate (dN/dE) of superflares versus flare energy (E) shows a power-law distribution with $dN/dE \propto E^{-\alpha}$, where $\alpha \sim 2$. It is interesting that this distribution is roughly similar to that for solar flares. In the case of the Sun-like stars (with surface temperature 5600–6000 K and slowly rotating with a period longer than 10 days), the occurrence rate of superflares with an energy of 10^{34}–10^{35} erg is once in 800–5000 yr. We also studied long-term (500 days) stellar brightness variation of these superflare stars and found that in some G-type dwarfs the occurrence rate of superflares was extremely high, ∼57 superflares in 500 days (i.e., once in 10 days). In the case of Sun-like stars, the most active stars show a frequency of one superflare (with 10^{34} erg) in 100 days. There is evidence that these superflare stars have extremely large starspots with a size about 10 times larger than that of the largest sunspot. We argue that the physical origin of the extremely high occurrence rate of superflares in these stars may be attributed to the existence of extremely large starspots.

Key words: stars: activity – stars: flare – stars: rotation – stars: solar-type – starspots

Online-only material: machine-readable table

1. INTRODUCTION

Flares are explosions on the stellar surface with intense release of the magnetic energy stored near starspots in the outer atmosphere of stars (e.g., Shibata & Yokoyama 2002; Gershberg 2005; Benz & Guedel 2010; Shibata & Magara 2011). During these flare events, various observable effects occur over a wide range in wavelength. On the Sun, our ability to spatially resolve the surface allows flares to be observed in rich detail with high cadence, and so much of our understanding of flare processes and their consequences come from observations of solar flares.

The typical total energy of a solar flare ranges from 10^{29} to 10^{32} erg (e.g., Shibata & Yokoyama 2002), and the duration is several minutes to several hours. There have been no observations of solar flares more energetic than 10^{32} erg. On the other hand, it is known that more such energetic flares occur on a variety of stars (Schaefer 1989; Landini et al. 1986). Schaefer et al. (2000) reported nine flare candidates on G-type dwarfs, i.e., solar-type stars (5100 K $\leqslant T_{\rm eff} <$ 6000 K and $\log g > 4.0$), with a total energy of 10^{33}–10^{38} erg, called superflares. The data sources of their study were, however, various and ambiguous (e.g., photography, X-ray, visual) and the number of discovered flares is so small that statistical properties, such as the frequency and energy distribution of superflares, are not well known.

Since solar flares lead to magnetic storms on the Earth, extensive damage may be caused in our civilization by large solar flares (e.g., Baker 2004). Geomagnetic storms induce electrical currents that can have a significant impact on electrical transmission equipment, leading to a widespread blackout. On 1989 March 13, in Quebec, Canada, 6 million people were without electric power for 9 hr as a result of a huge geomagnetic storm (Allen et al. 1989). Moreover, in 1859, our civilization experienced the largest flare on the Sun (∼10^{32} erg), called the Carrington flare after its discoverer (Carrington 1859), which caused the largest magnetic storm in the last 200 yr (Tsurutani et al. 2003), leading to a failure in the telegraph system all over Europe and North America (Loomis 1861).

Even solar flares of up to 10^{32} erg have strong effects on the Earth. If superflares were to occur on the Sun, our civilization would suffer from much more severe damages. Hence, it is very important to study the statistical properties of superflares on G-type dwarfs, especially to reveal whether superflares would really occur on Sun-like stars, which are defined as stars with surface temperatures of 5600 K $\leqslant T_{\rm eff} <$ 6000 K, surface gravity of $\log g > 4.0$, and rotational periods of $P > 10$ days. Recently, using *Kepler* data, Maehara et al. (2012) discovered 365 superflares (10^{33}–10^{36} erg) on 148 G-type dwarfs, which is much more than the 9 superflares on G-type dwarfs discovered by Schaefer et al. (2000). Among them, 14 superflares occurred on 10 Sun-like stars. Hence, Maehara et al. (2012) successfully analyzed the statistical properties of superflares on G-type dwarfs for the first time, revealing that

1. The occurrence rate of these superflares as a function of their total energy is quite similar to that of solar flares ($dN/dE \propto E^{-\alpha}$, $\alpha \sim 2$).
2. These superflare stars show quasi-periodic brightness variation, which may be evidence of very big starspots with stellar rotation.

3. It is found that superflares occur on Sun-like stars with frequency such that superflares with energy 10^{34}–10^{35} erg (100–1000 times of the largest solar flare) occur once in 800–5000 yr.
4. There is no hot Jupiter around these superflare stars, suggesting that hot Jupiters are rare in superflare stars.

Result (4) is important because Rubenstein & Schaefer (2000) suggested that G-type dwarfs with a hot Jupiter companion are good candidates for superflare stars. With this idea, they proposed that the Sun would never produce superflares since our Sun does not have a hot Jupiter. Result (4) suggests that their argument is not necessarily correct.

In spite of these new observations, Schaefer (2012) still argued that it was unlikely that superflares would occur on our present Sun. On the other hand, Shibata et al. (2013) concluded that we cannot reject the possibility that superflares of 10^{34}–10^{35} erg would also occur on our present Sun with a frequency of once in a few 1000 yr in view of the present theory of flares and dynamos.

The new observations of superflares by Maehara et al. (2012) renewed interest in the possibility of superflares on our Sun as well as on G-type dwarfs. The latter subject is important from the viewpoint of the habitability of exoplanets around G-type dwarfs.

The purpose of this paper is to study statistical properties of superflares on G-type dwarfs and Sun-like stars in more detail than before, extending the previous study by Maehara et al. (2012) (based on 120 days data) using longer-term (500 days) observational data in the *Kepler* mission. We found 1547 superflares on 279 G-type dwarfs and 44 superflares on 19 Sun-like stars, which is much more than what was discovered by Maehara et al. (2012); 365 superflares on 148 G-type dwarfs and 14 superflares on 10 Sun-like stars).

In Section 2, we describe the method of analysis, and in Section 3, we present typical light curves of superflares and the main results of our statistical analysis on occurrence rate. We also examined long-term brightness variation and superflares on the most active G-type dwarfs and Sun-like stars, and found remarkable results that superflares occur once in 10–100 days in these active stars. In Section 4, we discuss the physical implications of these results and compare these results with the time variation of solar flare occurrence rate as a function of solar activity level. Finally, in Appendix A, we show short-time cadence *Kepler* data for two typical superflares, and confirm that long-time cadence data grasp the basic properties of superflares.

2. METHOD

2.1. Kepler Data

Kepler carries an optical telescope with a 95 cm aperture and 105 deg^2 field-of-view (about 12° diameter), which is in Cygnus, Lyra, and Draco. This spacecraft was launched by NASA in Spring 2009 to search for exoplanets by finding planetary transit events, faint decreases in brightness due to a crossing planet. Since the orbiting planet is very small compared with the host star, the luminosity decrease from planetary transit is usually less than one-hundredth of the total brightness of the star. In addition, the planet passes in front of the star only when the orbit is nearly parallel with the line of sight. *Kepler* is, therefore, designed to obtain high-precision and long-period light curves of many stars. The typical precision is 0.1 mmag for a star of 12 mag and the number of observed stars is more than 160,000 (Koch et al. 2010). The time resolution is about 30 minutes and 1 minute. The resultant light curves are useful in detecting not only planetary transits but also other small brightness variations like stellar flares. In fact, there have been some previous studies of stellar flares using *Kepler* data (Walkowicz et al. 2011; Balona 2012), which focus on flares on early- or late-type stars.

Table 1
Length of the Observation Period During Each Quarter and Number of G-type Dwarfs

Quarter	N[a]	τ[b] (days)	Start Date (UT)	End Date (UT)
0	9511	10	2009 May 2	2009 May 11
1	75598	33	2009 May 13	2009 Jun 15
2	82811	89	2009 Jun 20	2009 Sep 16
3	82586	89	2009 Sep 18	2009 Dec 16
4	89188	90	2009 Dec 19	2010 Mar 19
5	86248	95	2010 Mar 20	2010 Jun 23
6	82052	90	2010 Jun 24	2010 Sep 22

Notes.
[a] Number of G-type dwarfs.
[b] Length of the observation period during each quarter.

2.2. Analysis Method

The data we used were taken during the period from 2009 May to 2010 September. We retrieved the data from the Multimission Archive at the Space Telescope Science Institute and analyzed the long-cadence (the time resolution is about 30 minutes) corrected flux of 9511, 75598, 82811, 82586, 89188, 86248, and 82052 stars in quarters 0, 1, 2, 3, 4, 5, and 6, respectively (all public light curves of G-type dwarfs observed by *Kepler*). The number of G-type dwarfs and monitoring period of each quarter are shown in Table 1. In Table 1, we also show the beginning and the end dates of each quarter, which are shown in the Kepler Data Release Notes.[5]

Since the aim of this study is to detect superflares on G-type dwarfs, we selected G-type dwarfs in all of the observed stars using the Kepler Input Catalog (Brown et al. 2011). The condition is 5100 K $\leqslant T_{\rm eff} <$ 6000 K and $\log g > 4.0$ and the number of selected stars is about 80,000 in 160,000.

There are various flare detection algorithms which detect flares from light curves (Osten et al. 2012; Walkowicz et al. 2011). In these algorithms, light curves are analyzed after they have detrended, and are searched for cases where the relative flux becomes statistically larger than a certain threshold for two or more times consecutively. The time resolution of the light curve of *Kepler* is about 30 minutes and some stars exhibit short periodic brightness variation (several hours). This period is comparable with the time scale of flare duration so that a detrending light curve has the potential to detrend the superflares themselves. To avoid misdetection of short stellar brightness variation and not overlook large flares, we calculated the distributions of brightness variation between all pairs of consecutive data points after creating light curves of all selected stars using the corrected flux in the data. The threshold of the flare was determined to be three times the value at the top 1% of the distribution. This threshold was chosen as a result of a test run so as not to misdetect other brightness variation. We also calculated the standard deviation of the distribution ($\sigma_{\rm diff}$) for defining the end time of a flare.

[5] http://archive.stsci.edu/kepler/data_release.html

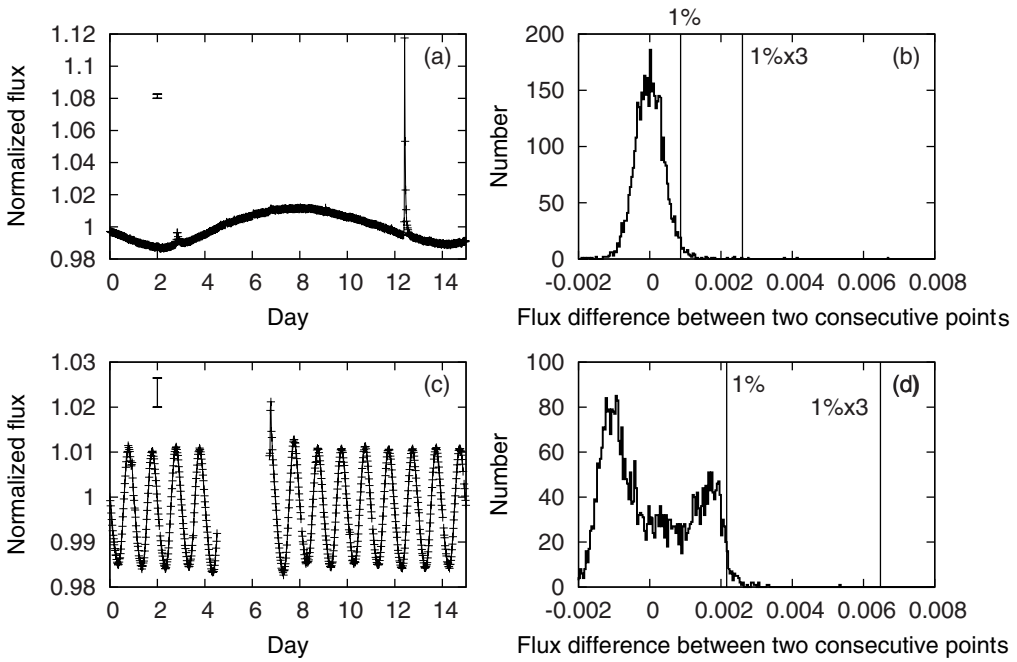

Figure 1. Explanatory figures of our flare-search method. The histograms in the right panels show the number distribution of brightness variation between all pairs of two consecutive data points. We set the threshold at three times the value at the top 1% of the distribution, and brightenings larger than the threshold are detected as flare candidates. Bars at $t = 2$ in the left panels correspond to the threshold determined by the right panels. (a) Light curve of KIC 9603367. (b) Histogram of the number distribution of the brightness difference between all pairs of two consecutive data points in (a). (c) Another example of light curve of KIC 4830001. (d) The same as (b), but for data in (c). Since the ordinary flux difference is much larger than in (b), only the flares with a much larger rising rate are detected. Panel (d) shows a distribution with two peaks, which correspond to the rates of typical increase and decrease in the brightness.

Figure 1 shows a schematic figure of our method. Figures 1(a) and (b) show a light curve of KIC 9603367 and the distribution of brightness variations between consecutive data points. Figures 1(c) and (d) are the same as (a) and (b) but for KIC 4830001. We show examples of the determination of threshold in the figures. Vertical lines in the right panels, written as "1%," correspond to the value of the top 1%, and the other vertical lines written as "1%×3" show the threshold of flare detection. Bars in the left panels at $t = 2$ days show the threshold determined by the right panels. Although the amplitudes of brightness variation of KIC 9603367 and KIC 4830001 are almost the same, the period of the brightness variation of KIC 9603367 (12.2 days) is longer than that of KIC 4830001 (1.0 days). Since the brightness variation between two consecutive observations in the stars with short-period variations (e.g., KIC 4830001) is larger than that of the stars with long-period variations (e.g., KIC 9603367), the distribution of brightness variations in short-period systems tend to spread wider than those of long-period systems, and the detection threshold of flares in short-period systems, therefore, becomes larger than that of flares in long-period systems. The detection threshold also depends on the amplitude of brightness variations. The thresholds in the stars showing large-amplitude variations tend to be larger than those in the small-amplitude systems.

The detection limit of this algorithm is determined from the value of the threshold divided by the average flux of the light curve. These detection limits are between 0.001 to 0.01 for most of our targets; therefore, flares are detected almost completely when the amplitudes are more than 1% of the average flux. The typical total energy of flare of 1% amplitude is 5×10^{34} erg.

The time at which the flux first exceeds the threshold is determined as the flare start time, and we removed long-term brightness variations around the flare by fitting with spline curves of three points. Here, three points are determined by the average of some data points just before the beginning of the flare and around 5 hr and 8 hr after the peak of the flare. After detrending, the flare end time was defined to be the time at which the flux residuals become smaller than $3\sigma_{\rm diff}$. We only analyzed flares with a duration longer than 0.05 days (at least two consecutive data points exceed the threshold) and excluded flare candidates with a shorter decline phase than the increase phase.

The pixel scale of the *Kepler* CCDs is about 4 arcsec and the typical photometric aperture for a 12 mag star contains about 30 pixels (van Cleve & Caldwell 2009). This suggests that the brightness variation of neighboring stars can affect the flux of the target star. If there is a flare star near the target and if large-amplitude flares occur on the flare star, *Kepler* can detect fake flares on the target star. In order to avoid these false events, we chose stars without neighboring stars within 12 arcsec for the analysis. The total number of samples that satisfy this condition was about 30%. The spatial distance between a pair of stars is calculated from the star properties in KIC. Superflares are rare events, therefore, the probability is very low that stars visually nearby exhibit superflares during the same 30 minute cadence. Such flare candidates are thought to be misdetected because of instrumental characteristics or contaminations of other sources. Although the reason for these instrumental characteristics is uncertain, light curves occasionally show discontinuity, which is thought to be caused by the variation of pointing accuracy or cosmic rays. Therefore, we excluded pairs of flares that occurred at the same time and whose spatial distance was less than 24 arcsec.

After removing the candidates of flares on neighboring stars, we checked light curves of flare candidates by eye, and examined the pixel level data of each G-type dwarf exhibiting flares by eye. Some contaminations of eclipsing binaries or transit events are found from light curves. If the spatial distribution of brightness

Table 2
Numbers of Flares, Flare Stars, and G-dwarfs

log P	$N_{\rm flare}$	$N_{\rm flarestar}$	$N_{\rm star}$	$N_{\rm star,old}$[a]
−1.0	2	1	38	34
−0.8	0	0	331	260
−0.6	1	1	219	156
−0.4	9	5	251	159
−0.2	35	12	334	215
0.0	34	12	393	299
0.2	65	20	422	428
0.4	127	29	656	870
0.6	120	27	1364	2000
0.8	75	16	3562	5549
1.0	28	8	9003	10248
1.2	102	13	19039	9338
1.4	27	3	30131	4919
1.6	0	0	17063	326

Note. [a] Period is calculated from the old data.

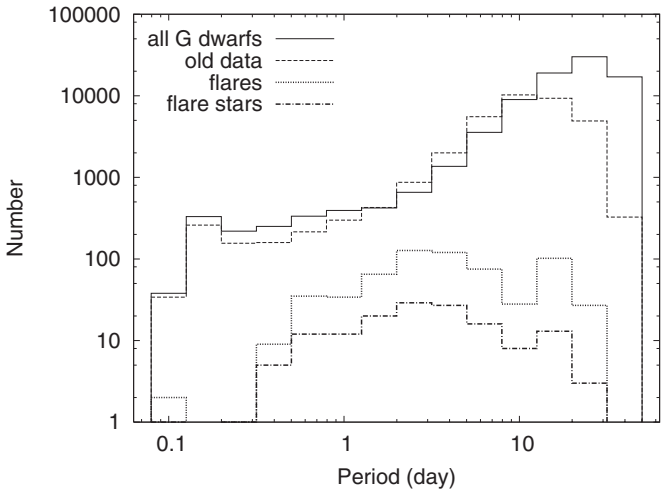

Figure 2. Number distributions of all G-type dwarfs (solid line), flare stars (dash–dotted line), and flares (dotted line) observed by *Kepler* as a function of rotational period. The periods of these stars are calculated from new data. We selected flares whose total energy are larger than 5×10^{34} erg. The dashed line indicates the distribution of period calculated from the old data, which is calibrated by the pipeline of the previous version.

on the CCDs is different between flares and at the quiescence, the flare is revealed to be a brightness variation of another source. A few percent and about 10% of flare candidates are removed by checking light curves and pixel level data, respectively.

We calculated periods of brightness variation from light curves, which correspond to the rotational period in the case of a single star with a dark spot. The variation period was calculated by the discrete Fourier transform method, and we chose the largest peak as the rotational period of the star when the peak was larger than the error level.

Figure 2 shows number distributions of all G-type dwarfs (solid line), flare stars (dash-dotted line), and flares (dotted line) observed by *Kepler* as a function of the rotational period. The periods of these stars are calculated from new data. A dashed line indicates the distribution of the period calculated from the old data, which is calibrated by the pipeline of the previous version. In this figure, we only selected flares whose total energy was more than 5×10^{34} erg. We obtained public data of releases 14 and 16 in this study. The dashed line shows the distribution of the period calculated from light curves from releases 4 to 9, which were used in Maehara et al. (2012). In releases 4 to 9, the data are calibrated using the old pipeline, and long-term brightness variation longer than 15 days tends to be removed (van Cleve et al. 2010). Hence, the number of stars with a period of more than 20 days was small (Table 2 and Figure 2). The reduction algorithm for the new *Kepler* data in releases 14 and 16 is improved (Jenkins et al. 2012; Stumpe et al. 2012). As a result, long-term brightness variation has been detected much more accurately than before, and more stars with a period of longer than 20 days are, therefore, detected from the new data (release 14 and 16) than from the old data (release 4–9). We chose 10 days as the threshold of Sun-like stars. A rotational period of 10 days corresponds to a radial velocity of $\sim$5 km s^{-1}, and this threshold is enough to distinguish slowly rotating stars from rapidly rotating stars (e.g., $v > 10$ km s^{-1}). This threshold is consistent with the threshold of "ordinary G-type dwarfs" in Schaefer et al. (2000).

2.3. Energy Estimation

We estimated the total energy of each flare from stellar luminosity, amplitude, and duration of flares by assuming that the spectrum of white-light flares can be described by a black-body radiation with an effective temperature of 10,000 K ($T_{\rm flare}$) (Mochnacki & Zirin 1980; Hawley & Fisher 1992). Assuming the effective temperature is 9000 K, the estimated energy becomes 66% of our result. This is the possible systematic uncertainty of our energy estimate.

Assuming that the star is a blackbody radiator, the bolometric flare luminosity ($L_{\rm flare}$) is calculated from $T_{\rm flare}$ and the area of flare ($A_{\rm flare}$) using the following equation,

$$L_{\rm flare} = \sigma_{\rm SB} T_{\rm flare}^4 A_{\rm flare}, \quad (1)$$

where $\sigma_{\rm SB}$ is the Stefan–Boltzmann constant. Since the star is not the blackbody radiator, this estimate is not accurate and may have an error of a few tens of percent. For the estimate of $A_{\rm flare}$ we use the observed[6] luminosity of the star ($L'_{\rm star}$), flare ($L'_{\rm flare}$), and flare amplitude of the light curve of *Kepler* after detrending ($C'_{\rm flare}$). These estimates are calculated from the following equations,

$$L'_{\rm star} = \int R_\lambda B_{\lambda(T_{\rm eff})} d\lambda \cdot \pi R_{\rm star}^2, \quad (2)$$

$$L'_{\rm flare} = \int R_\lambda B_{\lambda(T_{\rm flare})} d\lambda \cdot A_{\rm flare}, \text{ and} \quad (3)$$

$$C'_{\rm flare} = L'_{\rm flare} / L'_{\rm star}, \quad (4)$$

where λ is the wavelength, $B_{\lambda(T)}$ is the Plank function, and R_λ is the response function of the *Kepler* instrument. The instrument has a spectral bandpass from 400 nm to 850 nm (van Cleve & Caldwell 2009). We can estimate $A_{\rm flare}$ from these equations as

$$A_{\rm flare} = C'_{\rm flare} \pi R^2 \frac{\int R_\lambda B_{\lambda(T_{\rm eff})} d\lambda}{\int R_\lambda B_{\lambda(T_{\rm flare})} d\lambda}. \quad (5)$$

$L_{\rm flare}$ can be estimated from Equations (1) and (5), and $C'_{\rm flare}$ is a function of time; therefore, $L_{\rm flare}$ is also a function of time.

[6] These observed luminosities have an instrumental convolution factor.

Total bolometric energy of superflare ($E_{\rm flare}$) is an integral of $L_{\rm flare}$ during the flare duration,

$$E_{\rm flare} = \int_{\rm flare} L_{\rm flare}(t)dt. \quad (6)$$

According to Brown et al. (2011), $1-\sigma$ uncertainties of the stellar radius and the surface temperature in the Kepler Input Catalog are about ± 0.2 dex and ± 200 K, respectively. Hence, the uncertainty in the stellar luminosity can be estimated to be about $\pm 60\%$. Although the time cadence of the *Kepler* data was not sufficiently short to determine the peak and duration of flares, the uncertainties of the amplitude and duration of flares are much smaller than the uncertainty in the stellar luminosity because, when we calculate the flare energy, we integrate the brightness variation due to the flare over time from the start to the end of the flare. Therefore, total uncertainty in the flare energy is about $\pm 60\%$, and the occurrence rate of superflares in the unit energy range includes not only the counting error (the square root of the number of flares) but also the uncertainty of the flare energy.

3. RESULTS

3.1. Typical Example

We detected 1547 superflares on 279 G-type dwarfs, including 44 superflares on 19 Sun-like stars from the *Kepler* long-cadence data. The monitoring duration was about 500 days (quarters 0–6). Three hundred and sixty-five superflares were detected from 148 stars in a monitoring duration of about 120 days by Maehara et al. (2012). The number of superflares in this study is more than four times that of the previous study (Maehara et al. 2012), while the number of flare-generating stars is less than double. *Kepler* is monitoring the same stars and some active stars exhibit more than a few flares. One hundred and one superflare stars show only one superflare, while the number of superflare stars that exhibit more than one superflare is 178, and 8 Sun-like stars show more than one superflare in 19 Sun-like superflare stars. All flares are listed in Table 7 with parameters of stars and flares. BV Amp indicates the amplitude of stellar brightness variation in the quarter when the flare is detected. This value basically corresponds to the apparent fraction of the spot area to that of the disk. The definition of this value is as follows. We calculated $\Delta F(t)(= F(t) - F_{\rm av})$, where $F(t)$ is flux of light (stellar brightness) at date t and $F_{\rm av}$ is average flux. Then, excluding data points whose absolute values of ΔF are included in the top 1% of them, we calculated $(\max(\Delta F) - \min(\Delta F))/F_{\rm av}$, which is defined as BV Amp of the star in the quarter.

The numbers of detected superflares and stars that exhibit these flares are listed in Table 5. The fractions of superflare stars among all Sun-like stars, all G-type dwarfs, etc., are shown in Table 6 with numbers of flare stars and all observed stars in the category. In Figures 5 and 6, G-type dwarfs and Sun-like stars correspond to the lower right and middle left panels, respectively. Figure 3 shows four light curves of the most energetic superflares with *Kepler* ID, flare peak date, and total flare energy in the right panels (see Table 3 for detailed parameters of these stars.). Left panels indicate long-period light curves (30 days) and right panels show enlarged light curves of superflares during about a day. Vertical short lines in some left panels in Figure 3 show the time at which the flare is detected with our detection algorithm. Bars at $t = 2$ of left panels and $t = 0.1$ of right panels show the flare detection thresholds of the light curves.

Table 3
Parameters of Stars Illustrated in the Figures

Kepler ID	$T_{\rm eff}$[a] (K)	log g[b]	$R/R_\odot$[c]	KPmag[d]	$P_{\rm rot}$[e] (day)
4245449	5761	4.0	1.8	12.6	2.1
4543412	5907	4.3	1.3	11.2	2.2
6865484	5688	4.4	1.1	13.8	11.2
9574994	5925	4.4	1.1	15.1	12.3
10120296	5490	4.4	1.1	12.9	3.9
10422252	5118	4.2	1.3	13.6	5.2
10471412	5771	4.1	1.6	13.5	15.1
10524994	5747	4.5	1.0	15.3	12.0
12354328	5115	4.4	1.0	14.7	0.8

Notes.
[a] Effective temperature.
[b] Surface gravity.
[c] Stellar radius in units of solar radius.
[d] *Kepler* magnitude (Brown et al. 2011).
[e] Stellar rotation period estimated from brightness variation.

Various different periodic brightness variations are observed on many flare stars. These variations suggest the existence of large starspots on superflare stars (Rodono et al. 1986). There are, however, other mechanisms causing the brightness variation such as orbital motion of a binary system, eclipse by an accompanying star (Kopal 1959), or stellar pulsation. Here, stellar pulsation can be excluded because the pulsation period of the G-type dwarfs is shorter than a few hours (Unno et al. 1989). The possibility of the brightness variation being due to rotation must be carefully distinguished from its being a result of orbital motion, on the basis of the difference in the shape of the light curves (Debosscher et al. 2011). Figure 4 shows examples of superflares on Sun-like stars. The durations of the detected superflares are typically a few hours, and their amplitudes are generally of order $0.1 \sim 1\%$ of the stellar luminosity.

A major concern is the contamination from unresolved sources such as a low-mass companion. We discussed this topic in the supplementary information of Maehara et al. (2012) and concluded that most of the flares we detected are thought to be produced by G-type dwarfs because of the positive correlation between the amplitude of stellar brightness modulations and the flare frequency in Figure 5(b) of Maehara et al.'s (2012) supplementary information. Furthermore, our results show a dependence of flare occurrence rate on the effective temperature of the G-dwarfs (See Table 6). This dependence cannot be explained by the contamination from a low-mass companion.

3.2. Occurrence Rate of Superflares

Figure 5 represents the occurrence rate distributions of superflares. The configuration of this figure is basically the same as Figure 2 of Maehara et al. (2012) but the number of flares is more than four times that of the flares analyzed by Maehara et al. (2012). In Figure 5(a) we show the number of flares as a function of observed flare amplitude. The number of flares (N) is 1547, and the errors are estimated from the square root of the event number in each bin. Error bars from small number statistics are given by binomial distribution (Gehrels 1986); the error bars in figures, therefore, are overestimated when the number of flares is not large enough.

The average occurrence rate of superflares can be estimated from the number of observed superflares, the number of observed stars, and the length of the observational period. For

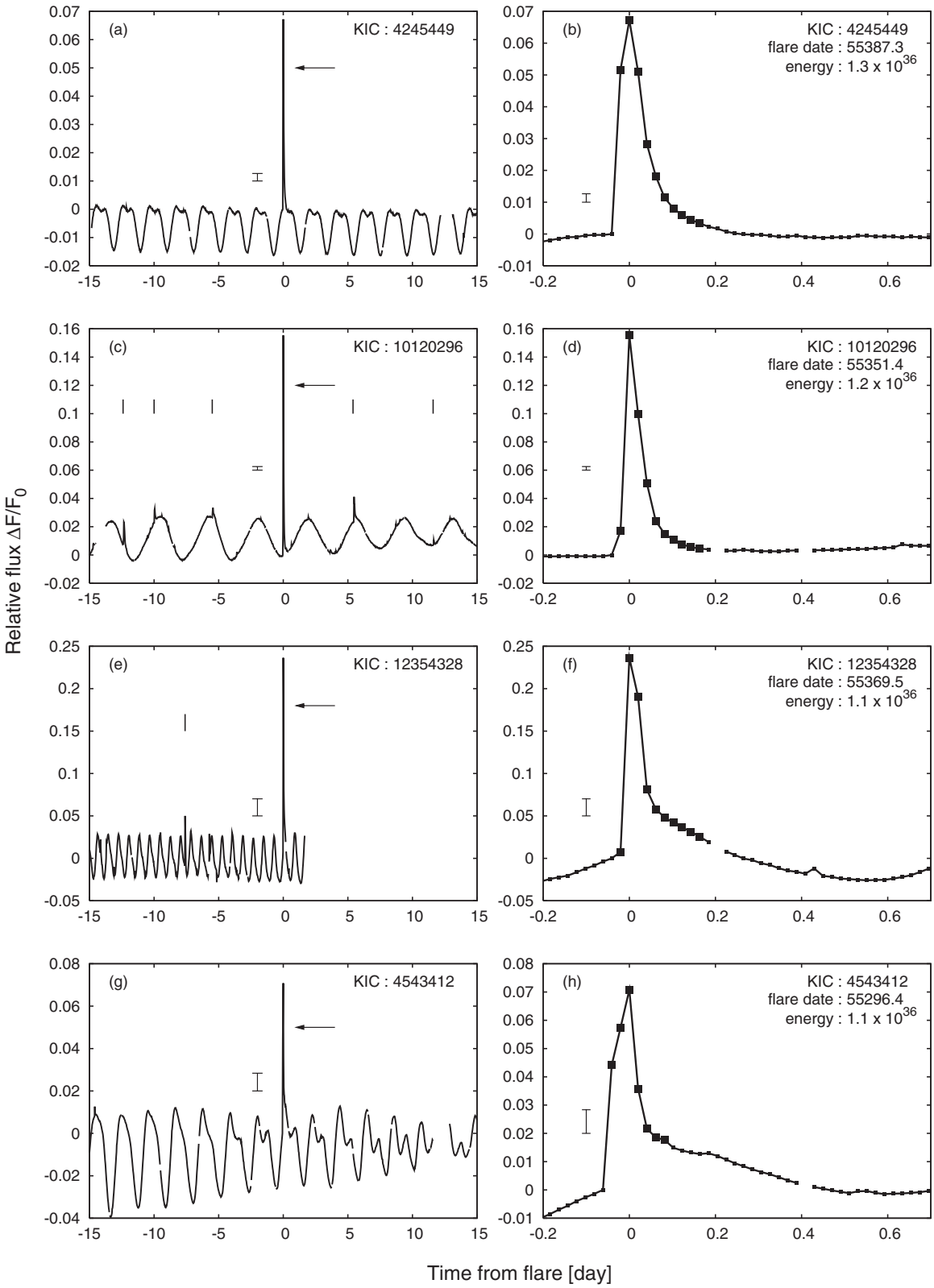

Figure 3. Light curves of the most energetic superflares. Horizontal and vertical axes correspond to days from the flare, and stellar brightness normalized by the brightness just before the flare (F_0), respectively. Panels on the left side show the 30 day time variation of stellar brightness, while panels on the right side show detailed brightness variation of a flare in a short period (0.9 days). Vertical short lines in some left panels show the time at which the flare was detected. Each bar with heads located just before the flare shows the detection threshold of superflare for the light curve. The star ID (*Kepler* ID), the Julian date of flare peak, and released total flare energy are shown in the upper right corner of figures in the right column.

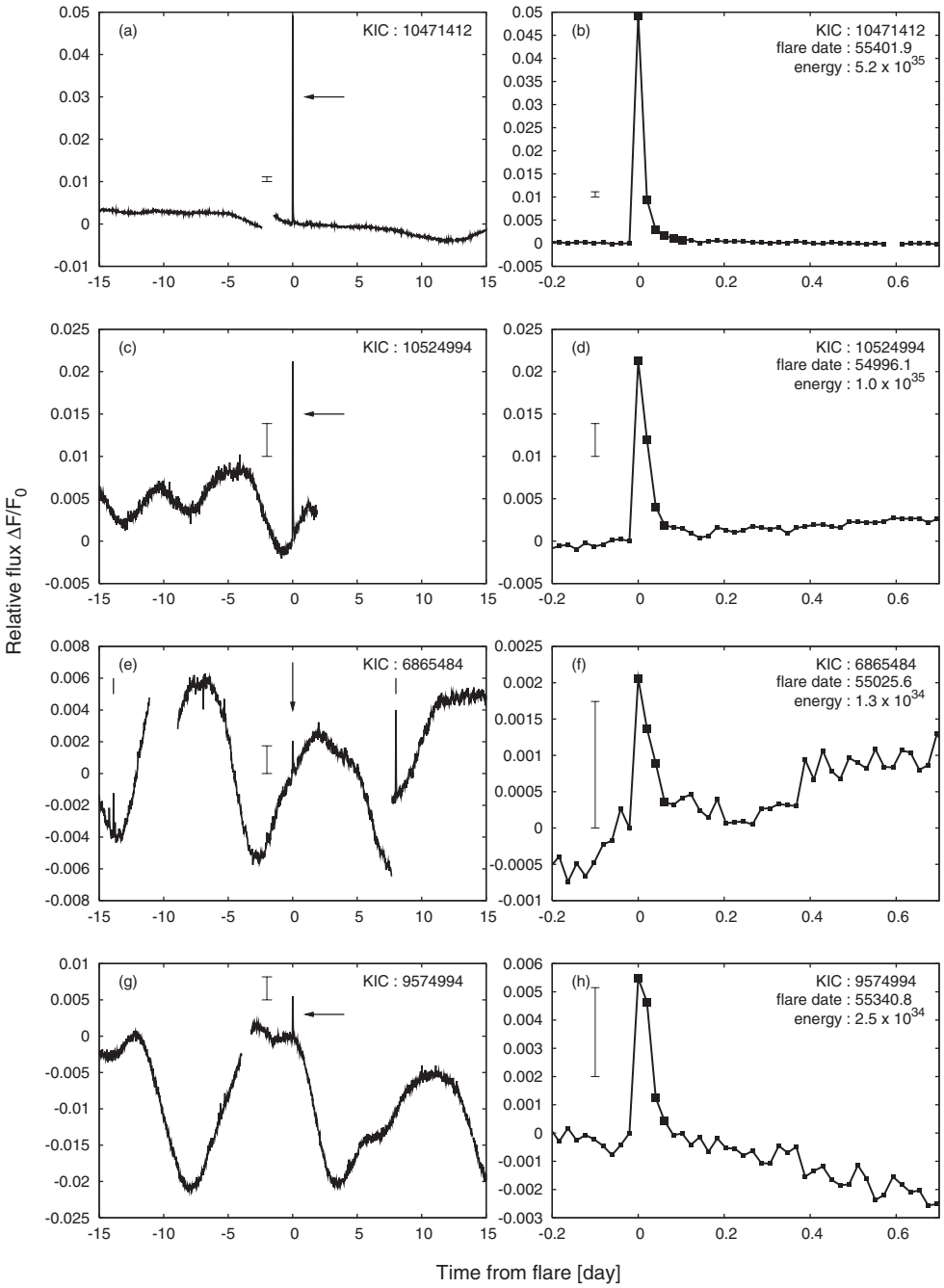

Figure 4. Same as Figure 3 but for the largest superflares on Sun-like stars (i.e., stars with a surface temperature 5600–6000 K and a rotational period longer than 10 days). The upper four panels show light curves of the most energetic superflare on Sun-like stars, while lower panels show superflares on Sun-like stars with a longer brightness variation period.

example, in the case of Sun-like stars, 44 superflares were detected from the data of about 14,000 stars over 500 days. Hence, the occurrence rate of superflares is 2.3×10^{-3} flares per year per star, which corresponds to a superflare occurring on a star once every 440^{+80}_{-60} yr. We show the frequency distributions of flares as a function of flare energy in Figures 5(b)–(d), but the sets of superflare-generating stars for each curve are different. The vertical axis indicates the number of superflares per star per year per unit energy. We show the distribution of all superflares (solid line) and superflares on slowly rotating (longer than 10 days period) stars (dashed line) in panel (b), superflares on all G-type dwarfs whose effective temperature ($T_{\rm eff}$) is 5100 K $\leqslant T_{\rm eff} <$ 5600 K (solid line) and $5600K \leqslant T_{\rm eff} < 6000K$ (dashed line) in panel (c), and slowly rotating G-type dwarfs of the same temperature range as (c) in panel (d). We show comparisons of this study and Maehara et al. (2012) in panels (e) and (f). Results of this study basically agree with the results in Maehara et al. (2012), and we can see reduced errors. It is seen from Figure 5(b) that the occurrence rate of superflares in all G-type dwarfs shows a power-law distribution

$$dN/dE \propto E^{-\alpha}$$

with $\alpha \simeq 2.2$ for all G-type dwarfs and $\alpha \simeq 2.0$ for flares on slowly rotating G-type dwarfs. It is interesting to note that

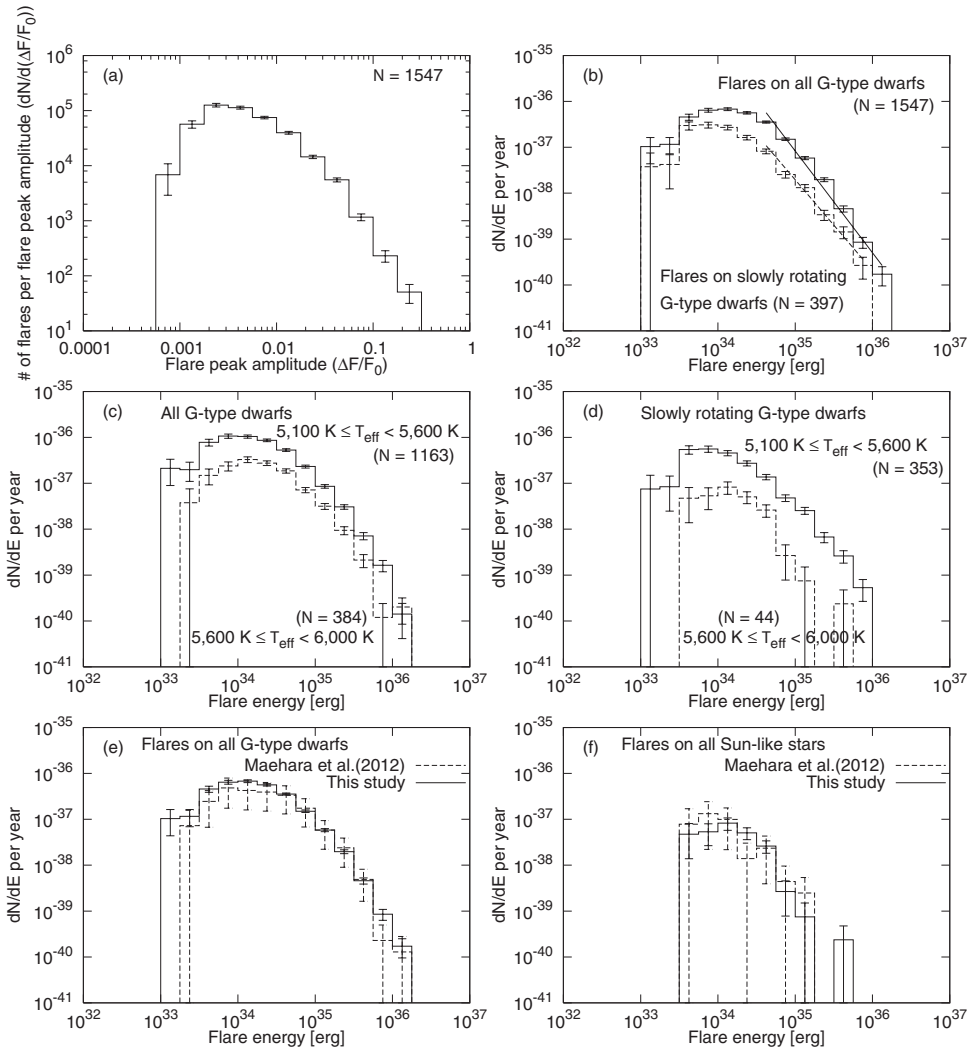

Figure 5. Frequency distribution of superflares on G-type dwarfs (5100 K $\leqslant T_{\rm eff} <$ 6000 K, and $\log g > 4.0$). (a) Number distribution of superflares as a function of the observed amplitude. The number of flares (N) is 1547. Note that the y-axis values have been divided by the bin width. (b) Frequency distribution of flares as a function of the flare energy. Solid and dashed lines show distributions on all stars and slowly rotating stars (the timescale of the brightness variation >10 days). The power-law index of all G-type dwarfs and slowly rotating G-type dwarfs is ∼2.2 and ∼2.0, respectively. (c) Same as (b) but for flares on all lower-temperature stars (5100 K $\leqslant T_{\rm eff} <$ 5600 K; solid line) and all high temperature stars (5600 K $\leqslant T_{\rm eff} <$ 6000 K; dashed line). (d) Same as (c) but only for flares on slowly rotating stars. (e), (f) Companions of the results in this study and Maehara et al. (2012). All errors are estimated to be a square root of the number of flares in each bin.

these distributions are quite similar to those for solar flares (e.g., Aschwanden et al. 2000) and stellar flares on red dwarfs (e.g., Shakhovskaia 1989).

We further found from Figures 5(b)–(d) that (1) the frequency of superflares on slowly rotating stars is smaller than that for all G-type dwarfs, and (2) the frequency of superflares on hot G-type dwarfs (5600 $< T_{\rm eff} <$ 6000 K) is smaller than that for cool G-type dwarfs (5100 $< T_{\rm eff} <$ 5500 K). These are basically the same results as those found in Maehara et al. (2012). The number of superflares on Sun-like stars is 36 on 13 stars, which is much more than the 14 superflares on 10 Sun-like stars found in Maehara et al. (2012). The occurrence rate distribution of superflares on these Sun-like stars is again similar to that for our Sun. The occurrence rate of superflares with energy of 10^{34} erg is once in 800 yr and once in 5000 yr for superflares with energy of 10^{35} erg.

3.3. Hot Jupiter

According to the *Kepler* candidate planet data explorer (Batalha et al. 2013), 2321 planets have been found in 1790 stars among 156,453 stars. Hence, the probability of finding exoplanets orbiting stars is about 1%. Howard et al. (2012) showed that the probability of finding a hot Jupiter was 0.5%. However, none of our superflare stars (279 G-type dwarfs) have a hot Jupiter according to the data explorer.

For a G-type dwarf with a hot Jupiter, the probability of a transit of the planet across the star is about 10% averaged over all possible orbital inclinations (Kane & von Braun 2008). If all of our 279 superflare stars are caused by a hot Jupiter as suggested by Rubenstein & Schaefer (2000), *Kepler* should detect 28 of them from transits. However, we did not find any hot Jupiters around our superflare stars as mentioned previously. This suggests that hot Jupiters associated with superflares are rare.

3.4. Occurrence Rate of Superflares on the Most Active Stars

Figure 6 represents the light curve of the most active superflare star (KIC10422252). This star exhibits 57 superflares in about 500 days, and hence the superflare occurrence rate is more than once in 10 days. The variation of the stellar

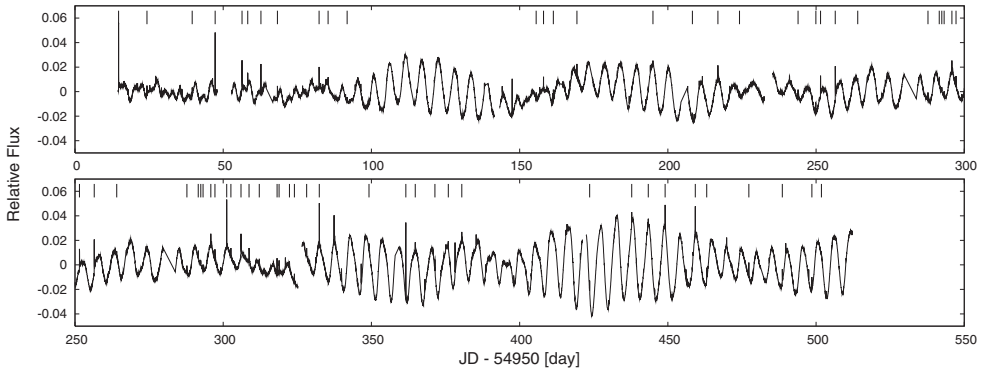

Figure 6. Long-term stellar brightness variations of KIC10422252. Vertical short lines indicate the peak time of the superflares we detected. The vertical axis shows the brightness variations relative to the average brightness.

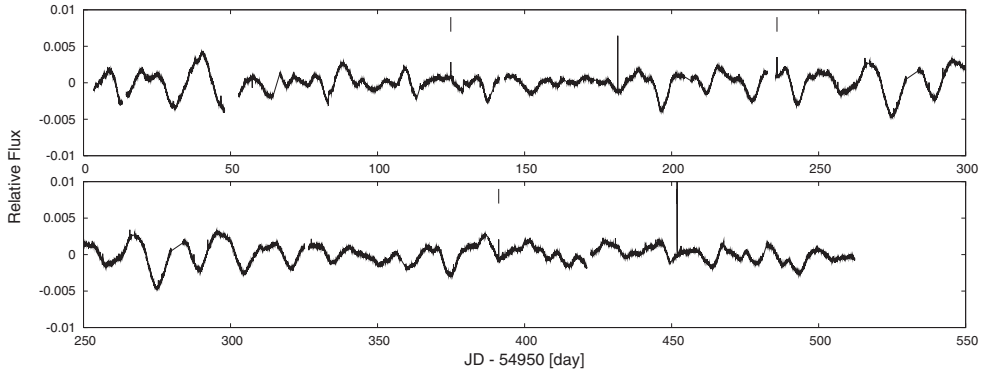

Figure 7. Same as Figure 6, but for KIC10471412. This star is similar to the Sun from a viewpoint of surface temperature, surface gravity, and rotational period. The rotational period of this star is estimated to be 15.1 days from the brightness variation of the light curve.

brightness contains modulation of the frequency which is different from but near the main frequency. Light curves of that sort are typically shown by the starspot system with differential rotation (Frasca et al. 2011).

Figure 7 is the same as Figure 6 but for KIC10471412. This star is an active Sun-like star, which produced four superflares over the course of the entire observation period (500 days). This occurrence rate of superflares corresponds to once in 100 days.

Figure 8 shows the flare occurrence rate distribution of the most active G-type dwarfs and Sun-like stars. The solid line corresponds to the average frequency of superflares on the 9 most active G-type dwarfs, whose superflare occurrence rate is more than once in 10 days. The dashed line shows the distribution for Sun-like stars that showed more than one superflare over the course of the entire observing period (about 500 days). Error bars are estimated from the square root of the numbers of superflares in each bin.

It is interesting to note that the frequency of superflares with $\sim 10^{34}$ erg in the dM4.5e star YZ CMi is once a month (Lacy et al. 1976; Kowalski et al. 2010), which is comparable to those of the most active G-dwarfs and Sun-like stars (once in 10–100 days).

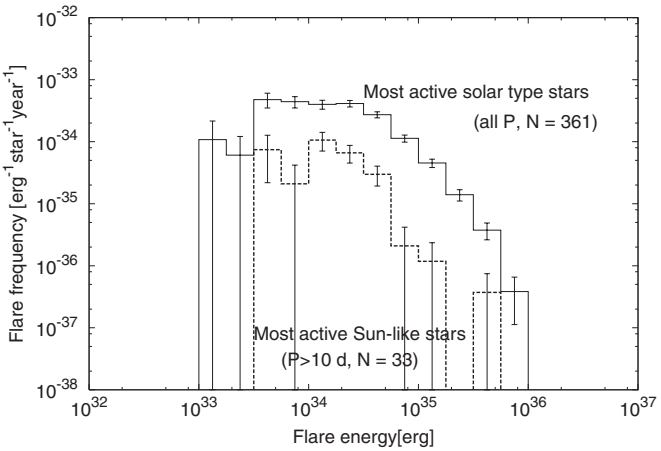

Figure 8. Same as Figure 5, but for most active G-type dwarfs (solid line), and most active Sun-like stars (dashed line). The most active G-type dwarf is defined as a G-type dwarf having a superflare occurrence rate greater than once in ~10 days. The most active Sun-like star is defined as a Sun-like star that exhibited more than one superflare over the course of the whole observation period.

4. DISCUSSION

4.1. Occurrence Rate Distribution of Superflares

We shall compare the occurrence rate distribution of superflares with those of solar flares and stellar flares on active G-type dwarfs discussed by Schrijver et al. (2012) in Figure 9. The solid-line histogram shows the flare occurrence rate distribution of superflares on G-type dwarfs and the dashed histogram corresponds to the frequency distribution of superflares on the most active G-type dwarfs. The error bars in the histogram represent the square root of event number in each bin. Solid lines indicate the frequency distribution of nanoflares observed in EUV (Aschwanden et al. 2000), microflares in soft X-rays (Shimizu 1995), and solar flares in hard X-rays (Crosby et al. 1993), respectively. The thin dot–dashed line shows a power-law line with the distribution $dN/dE \propto E^{-\alpha}$ with index $\alpha \sim 1.8$. The thick dotted line corresponds to the frequency distribution of stellar flare on active G-type dwarfs shown in Schrijver et al. (2012) (κ Cet, EK Dra, and 47 Cas). The frequency of flares on

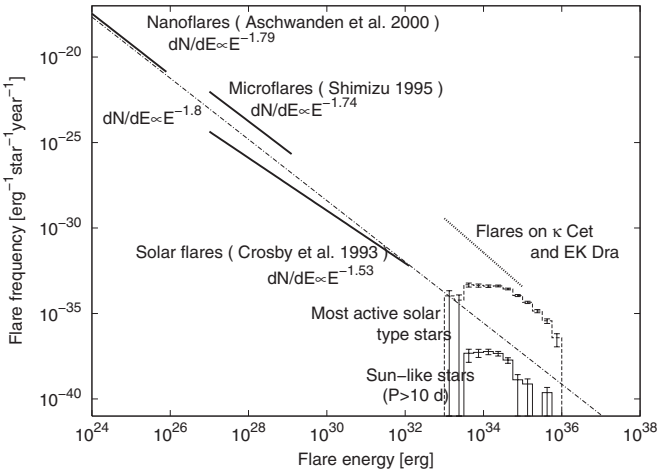

Figure 9. Occurrence rate of superflares on G-type dwarfs and of solar flares. The solid-line histogram shows the frequency distribution of superflares on Sun-like stars, while the occurrence rate of superflares on the most active G-type dwarfs (with flares more than once in about 10 days) is illustrated by the dashed line histogram. The error bars in the histogram are estimated from the square root of event number in each bin. The solid lines indicate the power-law distribution of solar flares observed in EUV (Aschwanden et al. 2000), soft X-rays (Shimizu 1995), and hard X-rays (Crosby et al. 1993), respectively. It is interesting that superflares in Sun-like stars, solar flares, microflares, and nanoflares are roughly on the same power-law line with an index of −1.8 (thin dash–dotted line) for a wide energy range from 10^{24} erg to 10^{35} erg.

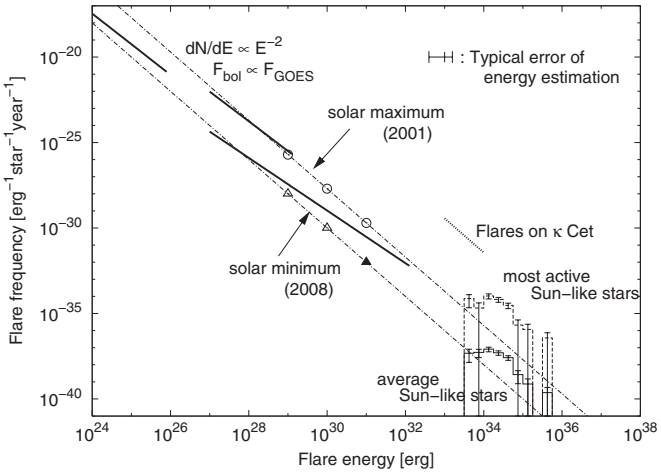

Figure 10. Flare occurrence rate as a function of the flare energy in light on the stellar activity cycle. Solid lines correspond to power-law distributions of solar flares, which are the same lines as in Figure 9. Distribution histograms represent the flare occurrence rate of superflares on all Sun-like stars (solid curve), and on Sun-like stars with more than one superflare (dashed curve). The bar at the upper right of this figure shows a typical error of our energy estimate. Dash–dotted lines correspond to power-law distributions estimated from numbers of solar flares observed by *GOES*. The flux in bolometric flux of flare ($F_{\rm bol}$) is estimated to be in proportion to the *GOES* X-ray Flux (F_{GOES}). We show the case of $F_{\rm bol} \propto F_{GOES}^{0.65}$ in Figure 13. Open circles show the occurrence rate of C-, M-, and X-class solar flares during the solar maximum, while frequency during the solar minimum is shown by triangles. No X-class solar flare was observed during the solar minimum (2008). We estimated the occurrence rate of X-class flares in the solar minimum, and the estimated frequency is shown by the closed triangle.

these G-type dwarfs is comparable to that of most active G-type dwarfs in our data. The maximum energy of these stellar flares is lower than that of superflares on the most active G-type dwarfs.

It is quite interesting to see that solar flares and superflares on Sun-like stars are roughly on the same power-law line. This suggests that the mechanism of superflares is similar to that of solar flares and microflares, because white-light flare energy is roughly in proportion to EUV and X-ray flare energy (but see Figure 13 for the case $F_{\rm white-light} \propto F_{\rm X-ray}^{0.65}$).

In Figure 10, we compare the frequency distribution of superflares on the most active Sun-like stars (the same curve as the dashed line of Figure 8) with those of solar flares and average Sun-like stars. It is found that the frequency of superflare occurrence in the most active Sun-like stars is about 1000 times larger than that of average Sun-like stars. In Figure 10, we also added the flare frequency in solar maximum (in 2001) and minimum (in 2008) using the statistics of solar flares based on *GOES* X-ray flux classification (X-class, M-class, C-class flares; see Table 4; T. T. Ishii et al. 2012, private communication). Here we assumed that the bolometric flux of flare ($F_{\rm bol}$) (70% white-light; Kretzschmar 2011) is in proportion to the *GOES* X-ray flux (F_{GOES}).[7] It is seen that the flare frequency in the solar maximum is larger than that in the solar minimum by a factor of about 200. It is also found that the superflare frequency curve in the most active Sun-like stars is well above that of solar flares during the maximum solar cycle. We can now understand from this figure that the difference in the activity level of the Sun (or sunspot number or total magnetic flux) leads to the difference in solar flare frequency in the different phases of the solar activity cycle.

This suggests that the total magnetic flux of the most active Sun-like stars is larger than that of the solar maximum. Since the total magnetic flux during the solar maximum and minimum are about 10^{24} Mx and 10^{23} Mx (e.g., Solanki et al. 2002; Vieira & Solanki 2010), the total magnetic flux in the most active Sun-like stars may be estimated to be $3 \times 10^{24} \sim 10^{25}$ Mx.

Table 4
Annual Variation of Number of Solar Flares Observed by *GOES*

Year	N_X[a]	N_M[a]	N_C[a]
1989	59	620	1929
1990	16	273	2262
1991	54	590	2653
1992	10	202	1922
1993	0	74	1142
1994	0	25	336
1995	0	11	148
1996	1	4	81
1997	3	21	286
1998	14	94	1188
1999	4	170	1854
2000	17	215	2223
2001	21	310	2101
2002	12	219	2323
2003	20	160	1316
2004	12	122	912
2005	18	103	599
2006	4	14	174
2007	0	10	73
2008	0	1	8
2009	0	0	28
2010	0	23	170
2011	8	111	1200

Notes. [a] Number of X-, M- and C-class flares.

[7] See Figure 12 and Appendix B for the case of flare energy estimated using Kretzschmar's (2011) empirical relation between the total solar irradiance and *GOES* X-ray flux of a solar flare.

Table 5
Number of Superflares and Superflare Stars

$T_{\rm eff}$	Slow[a]		Fast[a]		Total[a]	
	$N_{\rm flare}$[b]	$N_{\rm fstar}$[b]	$N_{\rm flare}$[b]	$N_{\rm fstar}$[b]	$N_{\rm flare}$[b]	$N_{\rm fstar}$[b]
5100–5600	353	50	810	133	1163	183
5600–6000	44	19	340	77	384	96
	497	69	1150	210	1547	279

Notes.
[a] Categorization by the P (stellar rotation period estimated from light curve). $P > 10$ days (Slow), $P < 10$ days (Fast) and the total of them (Total).
[b] Number of superflare ($N_{\rm flare}$) and number of flare stars in the category ($N_{\rm all}$).

Furthermore, we show the frequency of stellar flares on κ Cet with a thick dotted line in Figure 10. κ Cet is a G5-type main sequence star ($T_{\rm eff} = 5520$ K, $v \sin i = 3.9$ km s^{-1}, $P_{\rm rot} = 9.4$ days; Schrijver et al. 2012; Audard et al. 2000), and hence is slightly cooler than Sun-like stars. The frequency of flares on κ Cet is larger than that of the most active Sun-like stars by a factor of 100, although the maximum energy of flares on κ Cet (10^{34} erg) is lower than that of flares on the most active Sun-like stars (5×10^{35} erg).

Flare frequency of Sun-like stars is assumed to be determined by the average magnetic activity level of these stars. In Figure 10, it is interesting to see that the flare occurrence rate distribution of the average of all Sun-like stars is located between the solar maximum and minimum. This suggests that the average activity level of all Sun-like stars is comparable to that of the Sun. It is suggested from Figure 10 that Sun-like stars have a hyperactive cycle, when they exhibit 1000 times more flares than the average of Sun-like stars. The number of all Sun-like stars observed by *Kepler* is 14,410 and the number of hyperactive stars we detected was 6. The fraction of stars showing a hyperactive cycle is, therefore, of the order of 10^{-4}.

4.2. Dependence of Flare Frequency on Rotation of Superflare Stars

Rapidly rotating stars (rotational period: $P < 10$ days) tend to exhibit superflares more frequently than slowly rotating stars ($P > 10$ days) (see Tables 5 and 6). As mentioned in Section 2.2, the flare selection criteria, and therefore the detection completeness of flares, depends on the rotation period of the star. Our results show, however, that rapidly rotating stars show higher flare occurrence rate than slowly rotating stars. This trend cannot be affected by the nonuniformity of the detection completeness. The rotation period is correlated with the chromospheric activity, which is known to be an indicator of the magnetic activity of the stars (Noyes et al. 1984), and the rapidly rotating stars have higher magnetic activity than slowly rotating stars (Pallavicini et al. 1981). According to the dynamo theory of magnetic field generation, magnetic activity results from the interaction between rotation and convection (Parker 1979), and rapid rotation can cause high magnetic activity. Our result implies that rapidly rotating stars with higher magnetic activity can cause more frequent superflares.

The rotation period of a star is also known to be related to the stellar age and younger stars show more rapid rotation (Skumanich 1972; Barnes 2003). Our findings suggest that superflares occur more frequently on the young G-type dwarfs (i.e., rapidly rotating stars). Moreover, on G-type dwarfs similar in age to the Sun, superflares occur less frequently, though the maximum energy of superflares is nearly independent of rotation period (Maehara et al. 2012).

The relation between properties of superflares and the rotation period of superflare stars will be analyzed in detail in a future paper (Notsu et al. 2013b).

4.3. Superflares on the Sun?

It has been pointed out that there is no record of solar superflares over the past 2000 yr (Schaefer et al. 2000). According to the measurement of the impulsive nitrate events in polar ice, the largest proton flare event during the past 450 yr is the Carrington event (Shea et al. 2006), which occurred on 1859 September 1 (Carrington 1859). The total energy released in this flare was estimated to be on the order of 10^{32} erg (Tsurutani et al. 2003), which is only 1/1000 of the maximum energy of flares on the slowly rotating Sun-like stars we detected. Our criterion of rotation period for Sun-like stars is more than 10 days, and the average rotation period of Sun-like superflare stars is 12.7 days. This rotation period corresponds to a rotation velocity of $\sim$4 km s^{-1}. According to the rotation–age relation for single stars in Ayres (1997), this rotation velocity corresponds to an age of $\sim$1 Gyr. The rotational velocity of the Sun is $\sim$2 km s^{-1} (rotational period is 25 days) and the age of our Sun is 4.6 Gyr. Do superflares really occur on Sun-like stars most similar to the Sun which have a rotational period longer than 25 days? Table 7 shows 4 superflares (5.0×10^{34}, 2.4×10^{34}, 9.9×10^{33}, and 4.4×10^{34} erg) that occurred on Sun-like stars with surface temperatures of 5600 K $< T_{\rm eff} <$ 6000 K and rotational periods longer than 25 days. The number of such stars is about 5000 in our sample. This implies that superflares whose total energy is of the order of 10^{34} erg might occur on our Sun once in $\sim$2000 yr, although more detailed analysis is needed.

Table 6
Number of Superflare Stars and Observed Stars

$T_{\rm eff}$	Slow[a]			Fast[a]			Total[a]		
	$N_{\rm fstar}$[b]	$N_{\rm all}$[b]	$f_{\rm fstar}$[b]	$N_{\rm fstar}$[b]	$N_{\rm all}$[b]	$f_{\rm fstar}$[b]	$N_{\rm fstar}$[b]	$N_{\rm all}$[b]	$f_{\rm fstar}$[b]
5100–5600	50	14026	0.0036	133	1281	0.104	183	15307	0.012
5600–6000	19	14325	0.0013	77	1825	0.042	96	16150	0.0059
	69	28351	0.0024	210	3106	0.068	279	31457	0.0089

Notes.
[a] Categorization by P (stellar rotation period estimated from light curve). $P > 10$ days (slow), $P < 10$ days (fast) and the total of them (total).
[b] The number of flare stars ($N_{\rm fstar}$), the number of all observed G-type dwarfs ($N_{\rm all}$), and the fraction of stars that flare ($f_{\rm fstar} = N_{\rm fstar}/N_{\rm all}$) in the category.

Table 7
Parameters of Superflare Stars

Kepler ID	$T_{\rm eff}$[a] (K)	log g[b]	$R/R_{\odot}$[c]	KPmag	$P_{\rm rot}$[d] (day)	No. of flares
5522535	5732	4.3	1.3	13.8	20.3	1
6750902	5654	4.4	1.1	14.7	...	1
6865484	5688	4.4	1.1	13.8	11.2	12
7133671	5657	4.4	1.1	15.5	15.8	1
7354508	5714	4.4	1.1	13.4	17.0	1
7597685	5834	4.6	0.9	15.9	21.8	1
8212826	5811	4.2	1.4	14.0	26.3	2
8880526	5936	4.3	1.2	12.8	...	1
9574994	5925	4.4	1.1	15.1	12.3	1
9766237	5674	4.6	0.9	13.9	21.8	1
9944137	5725	4.6	0.8	13.8	25.3	1
10471412	5771	4.1	1.6	13.4	15.1	4
10524994	5747	4.5	1.0	15.3	12.0	5
11390058	5785	4.3	1.3	12.6	12.1	3
11401109	5732	4.5	0.9	14.5	29.1	1
11455711	5664	4.7	0.8	14.0	13.9	3
11494048	5929	4.4	1.1	13.4	14.9	1
11612371	5826	4.4	1.1	13.4	...	2
11961324	5750	4.4	1.1	14.2	...	2

Notes. All Sun-like stars are listed in the printed version of Table 7; additional parameters such as the total energy of flares are shown in the full version available in the online journal.
[a] Effective temperature.
[b] Surface gravity.
[c] Stellar radius in units of solar radius.
[d] Stellar rotation period estimated from brightness variation.

(This table is available in its entirety in a machine-readable form in the online journal. A portion is shown here for guidance regarding its form and content.)

It has also been proposed that hot Jupiters have an important effect on stellar magnetic activity (Rubenstein & Schaefer 2000; Cuntz et al. 2000; Ip et al. 2004) and that superflares occur only on G-type dwarfs with hot Jupiters. However, there is no hot Jupiter in our solar system. For these reasons, it was suggested that a superflare on the Sun was extremely unlikely (Schaefer et al. 2000; Rubenstein & Schaefer 2000).

We found, however, no hot Jupiters around the 279 G-type dwarfs with superflares (see Section 3.3). This suggests that a hot Jupiter is not a necessary condition for superflares. Recent theoretical research (Shibata et al. 2013) also suggested that G-type dwarfs can store enough magnetic energy to cause a superflare in the overshoot layer. Moreover, Miyake et al. (2012) reported an occurrence of an energetic cosmic-ray event in the eighth century recorded in a tree ring of Japanese cedar trees. There is a possibility that this event was produced by a superflare (with energy of $\sim 10^{35}$ erg) on our Sun.

In this paper, we found 1547 superflares on 279 G-type dwarfs in 500 days of *Kepler* data. Using these superflares, we calculated superflare occurrence rate distributions as a function of total superflare energy. This shows that power-law distributions and the power-law index were comparable to those of solar flares ($\sim$2), and the average occurrence rate of superflares with energy of 10^{34}–10^{35} erg is once in 800–5000 yr. According to the *Kepler* candidate planet data explorer, there was no host star of a hot Jupiter in all superflare stars. We showed a comparison of flare occurrence distributions of solar maximum, minimum, and superflare stars, and pointed out the existence of a hyperactive cycle of G-type dwarfs. We found hyperactive G-type superflare stars, which exhibit superflares more than once in 10 days. We found 36 superflares on Sun-like stars, and this is much more than the 14 superflares on Sun-like stars discovered by Maehara et al. (2012). Nevertheless, this number is still not enough to derive accurate statistical properties of superflares on Sun-like stars. This is important for discussion of the possibility of superflares on our present Sun. Hence, it will be important to continue to observe Sun-like stars for a longer time to increase the potential observation of superflares on Sun-like stars. It will also be important to get short-time (1 minute) cadence data to obtain information on small superflares (with energy of 10^{33}–10^{34} erg) which bridge the gap between superflares on Sun-like stars and the largest solar flares 3×10^{32} erg. *Kepler* only obtains photometric data. Rotational periods and areas of star spots calculated from them are an indirect estimate based on some presumptions. In order to get direct evidence of slow rotation, large spot, high activity, and binarity, high-dispersion spectroscopic observation is necessary. We have observed some superflare stars with the HDS on the Subaru telescope. The results from these observations will be reported elsewhere (Notsu et al. 2013a).

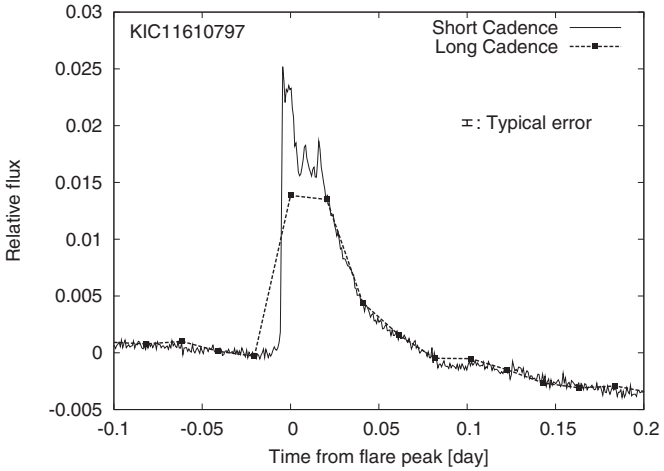

Figure 11. Light curves of a superflare on KIC11610797. Dashed and solid lines show the light curves of long and short time cadence data, respectively.

We are grateful to Professor Kazuhiro Sekiguchi (NAOJ) for useful suggestions. We also thank the anonymous referee for helpful comments. *Kepler* was selected as the 10th Discovery mission. Funding for this mission is provided by the NASA Science Mission Directorate. The data presented in this paper were obtained from the Multimission Archive at STScI. This work was supported by the Grant-in-Aid from the Ministry of Education, Culture, Sports, Science, and Technology of Japan (No. 25287039).

APPENDIX A

DETAILED LIGHT CURVE

We used light curves of long-time corrected flux (time resolution is about 30 minutes) to detect superflares. We can obtain the light curve of a flare with short time cadence data (1 minute) in some objects. We compared the estimated energy from long time data and short time data (details are shown in Section 2). Figure 11 shows the comparisons of the light curve of flare with long data and short data in KIC11610797. The estimated energy of a flare from long data is 1.4×10^{35} erg and from short data is 1.4×10^{35} erg. Figure 12 is the same as Figure 11, but for KIC 965268. The energy of a flare estimated from long data is 1.5×10^{34} erg and from short data is 1.9×10^{34} erg. Those values are in agreement within the error.

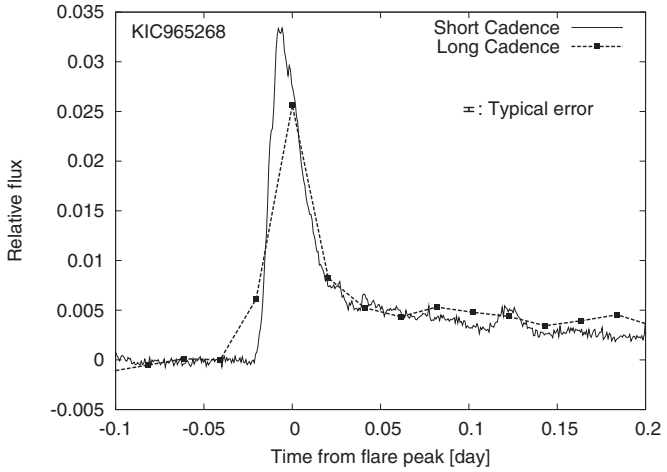

Figure 12. Same as Figure 11, but for KIC 9652680.

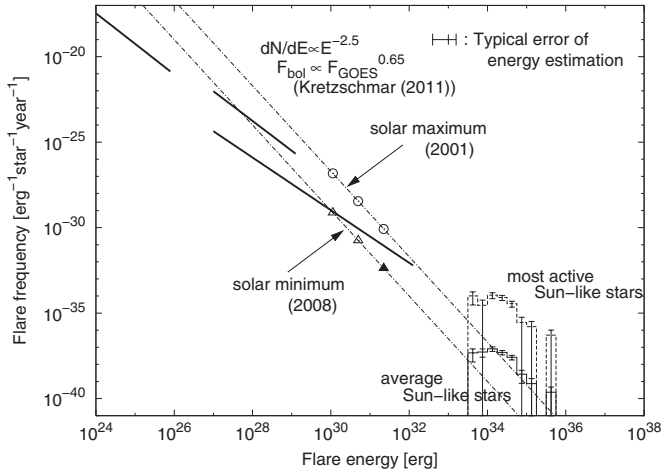

Figure 13. Same as Figure 10, but the total solar irradiance is estimated to be in proportion to the *GOES* X-ray flux to the power of 0.65 (Kretzschmar 2011).

Hence, we conclude the flare energies estimated from long time cadence data are reliable.

APPENDIX B

ESTIMATING TOTAL FLARE ENERGY FROM *GOES* X-RAY FLUX BASED ON KRETZSCHMAR'S RELATION

Kretzschmar (2011) derived the empirical relation between the bolometric flux of flare and *GOES* X-ray flux as

$$F_{\rm bol} = 2.4 \times 10^{12} F_{GOES}^{0.65}.$$

If we use this relation to derive the total flare energy from *GOES* X-ray flux assuming that the total energy of X10 class flare is 10^{32} erg, then the total energy of X-class, M-class, and C-class flares becomes $10^{31.4}$ erg, $10^{30.7}$ erg, and $10^{30.1}$ erg, respectively. Figure 13 is the same as Figure 10 but for the case of the flare energy estimate using Kretzschmar's relation. In this case, we clearly see disagreement between the observed frequency of nanoflares and those based on Kretzschmar's relation.

REFERENCES

Allen, J., Sauer, H., Frank, L., & Reiff, P. 1989, in Effects of the March 1989 Solar Activity, Vol. 70 (Eos Trans., AGU), 1479
Aschwanden, M. J., Tarbell, T. D., Nightingale, R. W., et al. 2000, ApJ, 535, 1047
Audard, M., Güdel, M., Drake, J. J., & Kashyap, V. L. 2000, ApJ, 541, 396
Ayres, T. R. 1997, JGR, 102, 1641
Baker, D. N. 2004, in Space Weather: The Physics Behind a Slogan, ed. K. Scherer, H. Fichtner, B. Heber, & U. Mall (Lecture Notes in Physics, Vol. 656; Berlin: Springer), 3
Balona, L. A. 2012, MNRAS, 423, 3420
Barnes, S. A. 2003, ApJ, 586, 464
Batalha, N. M., Rowe, J. F., Bryson, S. T., et al. 2013, ApJS, 204, 24
Benz, A. O., & Guedel, M. 2010, ARA&A, 48, 241
Brown, T. M., Latham, D. W., Everett, M. E., & Esquerdo, G. A. 2011, AJ, 142, 112
Carrington, R. 1859, MNRAS, 20, 13
Crosby, N. B., Aschwanden, M. J., & Dennis, B. R. 1993, SoPh, 143, 275
Cuntz, M., Saar, S. H., & Musielak, Z. E. 2000, ApJL, 533, L151
Debosscher, J., Blomme, J., Aerts, C., & De Ridder, J. 2011, A&A, 529, A89
Frasca, A., Fröhlich, H.-E., Bonanno, A., et al. 2011, A&A, 532, A81
Gehrels, N. 1986, ApJ, 303, 336
Gershberg, R. E. 2005, Solar-Type Activity in Main-Sequence Stars (Berlin: Springer)
Hawley, S. L., & Fisher, G. H. 1992, ApJS, 78, 565
Howard, A. W., Marcy, G. W., & Bryson, S. T. 2012, ApJS, 201, 15
Ip, W.-H., Kopp, A., & Hu, J.-H. 2004, ApJL, 602, L53
Jenkins, J., Caldwell, D., Thomas, B., et al. 2012, Kepler Data Release 14 Note, KSCI-19054
Kane, S. R., & von Braun, K. 2008, ApJ, 689, 492
Koch, D. G., Borucki, W. J., Basri, G., et al. 2010, ApJL, 713, L79
Kopal, Z. 1959, Close Binary Systems (London: Chapman & Hall), 147
Kowalski, A. F., Hawley, S. L., Holtzman, J. A., Wisniewski, J. P., & Hilton, E. J. 2010, ApJL, 714, L98
Kretzschmar, M. 2011, A&A, 530, A84
Lacy, C. H., Moffett, T. J., & Evans, D. S. 1976, ApJS, 30, 85
Landini, M., Fossi, B. C., Pallavicini, R., & Piro, L. 1986, A&A, 157, 217
Loomis, E. 1861, AmJS, 32, 318
Maehara, H., Shibayama, T., Notsu, S., et al. 2012, Natur, 485, 478
Miyake, F., Nagaya, K., Masuda, K., & Nakamura, T. 2012, Natur, 486, 240
Mochnacki, S. W., & Zirin, H. 1980, ApJL, 239, L27
Notsu, S., Honda, S., Notsu, Y., et al. 2013a, PASJ, 65, 112
Notsu, Y., Shibayama, T., Maehara, H., et al. 2013b, ApJ, 771, 127
Noyes, R. W., Hartmann, L. W., Baliunas, S. L., Duncan, D. K., & Vaughan, A. H. 1984, ApJ, 279, 763
Osten, R. A., Kowalski, A., Sahu, K., & Hawley, S. L. 2012, ApJ, 754, 4
Pallavicini, R., Golub, L., Rosner, R., et al. 1981, ApJ, 248, 279
Parker, E. N. 1979, Cosmical Magnetic Fields: Their Origin and Their Activity (Oxford: Oxford Univ. Press), 532
Rodono, M., Cutispoto, G., Pazzani, V., et al. 1986, A&A, 165, 135
Rubenstein, E. P., & Schaefer, B. E. 2000, ApJ, 529, 1031
Schaefer, B. E. 1989, ApJ, 337, 927
Schaefer, B. E. 2012, Natur, 485, 456
Schaefer, B. E., King, J. R., & Deliyannis, C. P. 2000, ApJ, 529, 1026
Schrijver, C. J., Beer, J., Cliver, E. W., et al. 2012, JGRA, 117, 08103
Shakhovskaia, N. I. 1989, SoPh, 121, 375
Shea, M. A., Smart, D. F., McCracken, K. G., Dreschhoff, G. A. M., & Spence, H. E. 2006, AdSpR, 38, 234
Shibata, K., Isobe, H., Hillier, A., et al. 2013, PASJ, 65, 49
Shibata, K., & Magara, T. 2011, LRSP, 8, 6
Shibata, K., & Yokoyama, T. 2002, ApJ, 577, 422
Shimizu, T. 1995, PASJ, 47, 251
Skumanich, A. 1972, ApJ, 171, 565
Solanki, S. K., Schuessler, M., & Fligge, M. 2002, A&A, 383, 706
Stumpe, M. C., Smith, J. C., Van Cleve, J. E., et al. 2012, PASP, 124, 985
Tsurutani, B. T., Gonzalez, W. D., Lakhina, G. S., & Alex, S. 2003, JGR, 108, 1268
Unno, W., Osaki, Y., Ando, H., Saio, H., & Shibahashi, H. 1989, Nonradial Oscillations of Stars (Tokyo: Univ. Tokyo Press), 237
van Cleve, J. E., & Caldwell, D. A. 2009, Kepler Instrument Handbook, KSCI-19033
van Cleve, J. E., Jenkins, J., Caldwell, D. A., et al. 2010, Kepler Data Release 3 note, KSCI-19043
Vieira, L. E. A., & Solanki, S. K. 2010, A&A, 509, A100
Walkowicz, L. M., Basri, G., Batalha, N., et al. 2011, AJ, 141, 50